

UCSF

UC San Francisco Previously Published Works

Title

Molecular insights into the binding interactions and energetics of the omicron spike variant with hACE2 and a neutralizing antibody

Permalink

<https://escholarship.org/uc/item/6b72p7fm>

Journal

Journal of Structural Biology, 216(2)

ISSN

1047-8477

Authors

Kumar, Vipul
Shefrin, Seyad
Sundar, Durai

Publication Date

2024-06-01

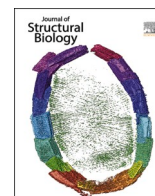
DOI

10.1016/j.jsb.2024.108087

Copyright Information

This work is made available under the terms of a Creative Commons Attribution License, available at <https://creativecommons.org/licenses/by/4.0/>

Peer reviewed



Research Article

Molecular insights into the binding interactions and energetics of the omicron spike variant with hACE2 and a neutralizing antibody

Vipul Kumar¹, Seyad Shefrin, Durai Sundar^{*}

Department of Biochemical Engineering and Biotechnology, Indian Institute of Technology (IIT) Delhi, New Delhi 110016, India



ARTICLE INFO

Edited by Elka Georgieva

Keywords:

Molecular dynamics simulation
SARS-CoV2
Receptor binding domain
Modelled mutants

ABSTRACT

The global spread of Severe Acute Respiratory Syndrome Coronavirus 2 (SARS-CoV-2) since 2019 has led to a continuous evolution of viral variants, with the latest concern being the Omicron (B.1.1.529) variant. In this study, classical molecular dynamics simulations were conducted to elucidate the biophysical aspects of the Omicron spike protein's receptor-binding domain (RBD) in its interaction with human angiotensin-converting enzyme 2 (hACE2) and a neutralizing antibody, comparing it to the wildtype (WT). To model the Omicron variant, 15 in silico mutations were introduced in the RBD region of WT (retrieved from PDB). The simulations of WT spike-hACE2 and Omicron spike-hACE2 complexes revealed comparable binding stability and dynamics. Notably, the Q493R mutation in the Omicron spike increased interactions with hACE2, particularly with ASP38 and ASP355. Additionally, mutations such as N417K, T478K, and Y505H contributed to enhanced structural stability in the Omicron variant. Conversely, when comparing WT with Omicron in complex with a neutralizing antibody, simulation results demonstrated poorer binding dynamics and stability for the Omicron variant. The E484K mutation significantly decreased binding interactions, resulting in an overall decrease in binding energy (~ -57 kcal/mol) compared to WT (~ -84 kcal/mol). This study provides valuable molecular insights into the heightened infectivity of the Omicron variant, shedding light on the specific mutations influencing its interactions with hACE2 and neutralizing antibodies.

1. Introduction

The severe acute respiratory syndrome coronavirus-2 (SARS-CoV-2) originated in the Wuhan province of China in December 2019, causing Coronavirus Disease-19 (COVID-19), which has taken millions of lives till now (Lu et al., 2020). The SARS-CoV-2 is highly similar to the previously known SARS-CoV that caused the outbreak in 2002 and 2004 (Abdelrahman et al., 2020; Boni et al., 2020). The SARS-CoV-2 originated in China in December 2019 and was transmitted globally within a couple of months; therefore, it was declared a pandemic by WHO in March 2020 (Cucinotta and Vanelli, 2020; Ranney et al., 2020). Coronaviruses are the enveloped single-stranded, +sense RNA viruses (V'Kovski et al., 2021). There are four similar Coronaviruses that have been known for human infections, namely, Alpha (NL63 and 229E) and Beta (HKU1 and OC43) (Ye et al., 2020). All these viruses are reported to have zoonotic origin (Ye et al., 2020). Since the SARS-CoV-2 virus outbreak, this virus has been mutating and giving rise to various variants (Krause et al., 2021; Kumar et al., 2021; Singh et al., 2021). Moreover,

the fast and rapid mutation rates in the SARS-CoV-2 are the primary concern for the global medical systems (Zeyaullah et al., 2021). Currently, eight vaccines are commercially available around the globe and have been approved by the WHO (<https://covid19.trackvaccines.org/agency/who/>). Most vaccines are based on the spike protein of the SARS-CoV-2 (Heinz and Stiasny, 2021). Until now, Paxlovid, Remdesivir and Molnupiravir have been approved by WHO for the treatment of COVID-19 (Kalra et al., 2020; Kalra et al., 2021). Nevertheless, the critical question remains: given the rapid mutation in the SARS-CoV-2, mainly in the spike region, would these available vaccines and medicine be effective against the coming new variants?

Based on the combinations, number of mutations and the effects of these mutations in transmissibility, virulence, and effectiveness of the available therapeutics against these, WHO has categorized these variants into three categories. As of now, there are five variants of concerns (VOC), namely, B.1.1.7 (Alpha), B.1.351 (Beta), P.1 (Gamma), B.1.617.2 (Delta) and B.1.1.529 (Omicron) (Kumar et al., 2021; Callaway and Ledford, 2021) (<https://www.who.int/en/activities/tracking-SARS->

^{*} Corresponding author at: Department of Biochemical Engineering and Biotechnology, Indian Institute of Technology (IIT) Delhi, New Delhi 110016, India. E-mail addresses: vipul2732@gmail.com (V. Kumar), bez188440@dbeb.iitd.ac.in (S. Shefrin), sundar@dbeb.iitd.ac.in (D. Sundar).

¹ Present Address: Department of Bioengineering and Therapeutic Sciences, University of California San Francisco, San Francisco, CA 94143, USA.

CoV-2-variants/). Further, there are two variants of Interest (VOI), C.37 (Lambda) and B.1.621 (Mu). Moreover, there are seven Variants under monitoring (VUM), AZ.5, C.1.2, B.1.617.1, B.1.526, B.1.525, B.1.630, B.1.630 and B.1.640 (naming is according to Pango lineage) (<https://www.who.int/en/activities/tracking-SARS-CoV-2-variants/>). The most recent outbreak has been reported in South Africa due to the Omicron variant of SARS-CoV-2 (Callaway and Ledford, 2021). And on November 26, 2021, WHO considered this variant Variant of Concern (<https://www.who.int/en/activities/tracking-SARS-CoV-2-variants/>). This new variant has 32 mutations in the spike protein only, including at the Receptor Binding Domain (RBD) and furin cleavage site (Chen et al., 2021). It is also reported that this variant has 69–70 deletions in the S gene region, leading to S gene dropout or S gene target failure in the RT-PCR tests. However, this can be used as a marker for the identification of this particular variant (Venkatakrishnan et al., 2021; Karim and Karim, 2021) ([https://www.who.int/news/item/26-11-2021-classification-of-Omicron-\(b.1.1.529\)-sars-cov-2-variant-of-concern](https://www.who.int/news/item/26-11-2021-classification-of-Omicron-(b.1.1.529)-sars-cov-2-variant-of-concern)). The mutation profile in the Omicron spike RBD domain is shown in Fig. 1.

Given the severity and continuous mutation profile in SARS-CoV2, it was important to study these mutations in the Omicron variant carefully. Such a study will aid in understanding the impact of these mutations on the structure, function, and interactions, particularly regarding

the spike protein's binding to Angiotensin-converting enzyme 2 (hACE2) and antibodies. Therefore, the aim of this study was to investigate the binding, dynamics and energetics of the WT with and neutralizing antibody and compare them with Omicron. For this study, the 2.45 Å resolution crystal structure of WT spike bound with hACE2 (PDB ID: 6MOJ) and WT spike bound with neutralizing antibody (PDB ID: 7BWJ) was used. The focus was on the mutation profile of the spike in the RBD domain. The Omicron spike variant was modelled by inducing 15 mutations (G339D, S371L, S373P, N417K, N440K, G446S, S375F, S477N, T478K, E484K, Q493R, G496S, Q498R, N501Y and Y505H) in the WT spike RBD for both the complexes (with hACE2 and neutralizing antibody). A 200 ns classical MD simulation was carried out to study the spike variant's interaction pattern, dynamics and energetics. It was found that in the case of spike-hACE2, mutations in the Omicron variant caused an increase in binding interactions with hACE2; at the same time, some of these mutations were also found to be energetically favorable, making the omicron structure more stable. On the other hand, the mutation in the Omicron variant caused a significant reduction in contacts and binding energy with neutralizing antibody. Our analysis showed that the Omicron variant enables a higher binding of the spike RBD with hACE2 than the WT and reduces the binding with neutralizing antibody. The results of these computational analyses give

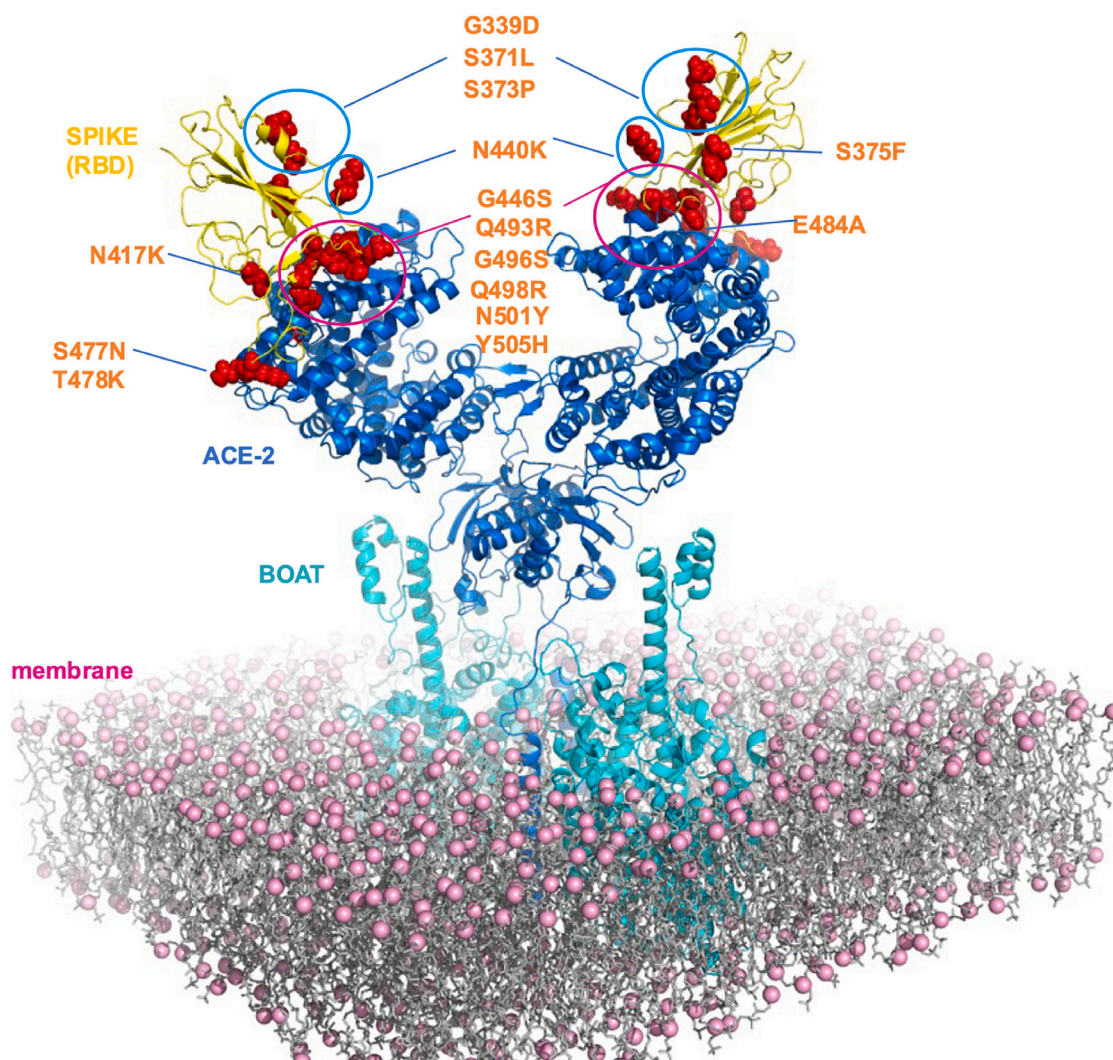


Fig. 1. The mutations in the Omicron variant in the spike (Receptor Binding Domain) bound with hACE2. The pictorial representation of spike RBD (Yellow colour), with hACE2 (Blue colour) and BOAT (SLC6A19) (Cyan colour) Complex in a Bilayer (PDB ID: 6 M17). The red spheres in the spike RBD region showing the 15 mutations reported in the Omicron variant. For this study, only the spike (RBD) complexed with hACE2 has been considered. (For interpretation of the references to colour in this figure legend, the reader is referred to the web version of this article.)

insights about the higher transmissibility of the Omicron variant and its virulence potential compared to the WT SARS-Cov2.

2. Material and methods

2.1. Molecular dynamics (MD) simulations

A similar method for other systems has been reported in detail elsewhere (Kumar et al., 2021). Here, we have briefly reported the overall methods utilized. For this study, only the spike (RBD) complexed with hACE2 has been considered. The 3D X-ray crystal structures of wildtype spike protein (RBD) bound with hACE2 and neutralizing antibody were retrieved from Protein Data Bank (PDB) having PDB ID 6M0J (resolution 2.45 Å) and 7BWJ (resolution 2.85 Å), respectively. The retrieved complexes were then prepared in the following three steps for the simulation using the protein preparation wizard of Schrodinger software (Schrödinger Release, 2020-2). Firstly, complexes were pre-processed by adding missing hydrogens, filling missing side chains, filling missing loops and removing water. Secondly, pre-processed structures were optimized for correct hydrogen bond assignment using PROPKA tool of the Protein preparation wizard at pH 7 (Olsson et al., 2011). Finally, the optimized structures were restrained minimized until heavy atoms converged to RMSD 0.30 Å using OPLS3e forcefield (Roos et al., 2019). After the preparation, in both the complexes (spike-hACE2 and spike-Antibody), 15 mutations (Fig. 1), which were reported for the Omicron variant was introduced in the RBD domain of the spike protein using the Maestro suite of Schrodinger (Schrödinger Release, 2020-2; Madhavi Sastry et al., 2013). Then, the mutated complexes were subjected to the 50 ns of the classical MD simulations, and the final structure files were then taken as the initial prepared structure. Finally, all the initial prepared structure complexes (WT and mutated) were taken for the system building for the MD simulation. Systems were built using the TIP3P water model (Jorgensen et al., 1983) and neutralized by the addition of appropriate Na⁺/Cl⁻ ions. Further, the built systems were minimized by running 100 ps low-temperature (10 K) Brownian motion MD simulation (NVT ensemble). Then, the minimized systems were subjected to the following five steps of the system relaxation protocol before simulation. (i) Brownian dynamics (NVT) at temperature 10 K with restraints on solute-heavy atoms for 100 ps. (ii) Classical MD simulation in NVT ensemble at temperature 10 K with restraints on solute heavy atoms for 12 ps. (iii) Classical MD in NPT ensemble at temperature 10 K with restraints on solute heavy atoms for 12 ps. (iv) Classical MD in NPT ensemble at temperature 300 K with restraints on solute heavy atoms for 12 ps and (v) Classical MD in NPT ensemble at temperature 300 K without any restraints for 24 ps. Finally, the relaxed systems were subjected to 200 ns classical unrestrained MD simulations in an NPT ensemble at 300 K temperature maintained by Nose-Hoover chain thermostat constant pressure of 1 atm maintained by Martyna-Tobias-Klein barostat and an integration time step of 2 fs with a recording interval of 200 ps, having coulombic short-range interaction radius cut-off of 9.0 Å and custom initial velocity randomization value (2007) (Schrödinger Release, 2020-2).

2.2. MD simulation analysis

The MD trajectories were analyzed for the Root Mean Square Deviation (RMSD), Root Mean Square Fluctuation (RMSF) and number of hydrogen bonds between the complexes using the Simulation event analysis tool of Desmond integrated with Maestro suite of Schrodinger Software. Further, the hydrogen bond occupancy was calculated using visual molecular dynamics (VMD) (Humphrey et al., 1996). The molecular mechanics generalized Born surface area (MM/GBSA) free binding energy between spike proteins and hACE2, along with spike protein and neutralizing antibody, was calculated for the 20 structures extracted from the 100 ns–200 ns MD trajectory using the prime module of Schrodinger software (Schrödinger Release, 2020-2). Finally, the

energy contribution of the mutated residues was compared with wild-type residues using the Prime module of Schrodinger. The detailed mathematical equations and theory behind these calculations have been reported elsewhere (Kumar et al., 2021).

3. Results

3.1. Modelled mutant omicron spike (RBD) had similar dynamics as WT, while significantly increased the number and fraction of H-bond interactions with hACE2

The wildtype (WT) spike (RBD)-hACE2 complex, along with the Omicron spike (RBD)-hACE2 complex were simulated for the 200 ns. Firstly, the global deviation of the complexes with time was analyzed by calculating the RMSD. The RMSD data showed that within the first 20 ns of the simulation, both the complexes got stabilized, and both had similar average deviation throughout the simulations afterward, i.e., WT-spike-hACE2 (3.07 ± 0.41 Å) and Omicron-spike-hACE2 (3.27 ± 0.40 Å) (Fig. 2A). When the average fluctuation of the individual residues of the WT spike and Omicron spike protein was analyzed through RMSF calculation, it was found that Omicron spike residues were less dynamic than the WT spike. The average RMSF of the WT spike was 3.26 ± 1.22 Å, while for the Omicron spike it was 2.90 ± 0.93 Å. It was also observed that although Omicron's overall spike RBD residues had less fluctuation than WT, residues (475–493) of Omicron had higher fluctuation than WT (Fig. 2B). After analyzing the overall deviation and average residue fluctuation throughout the 200 ns simulation time, it was observed that there was not a significant difference between the two complexes in terms of dynamics. Then, the number of hydrogen bonds between the spike-hACE2 in both the modelled mutants and the wild type was calculated. It was found that WT spike-hACE2 (11.23 ± 2.12) had a higher number of hydrogen bonds throughout the simulations than the Omicron spike-hACE2 (8.07 ± 1.75) (Fig. 2C). Further, MM/GBSA free binding energy of the spike-hACE2 complex was computed by extracting 20 structures from the equal interval from the last 100 ns of the simulations. The binding free energy of each of the 20 structure complexes has been shown in Fig. 2D. The individual binding energy for each frame along with all the energy terms contributing to overall MM/GBSA binding free energy has been reported in supplementary material (Table S1). The average free binding energy showed that both Omicron-spike-hACE2 (-103 ± 17 kcal/mol) and WT-spike-hACE2 (-100 ± 14 kcal/mol) complexes had similar binding affinity for hACE2. Then, the significant (>20 % of simulation time) hydrogen bonding residues of spike protein with hACE2 and their contact frequency were calculated. The Omicron spike variant had more significant hydrogen bonding with hACE2 than the WT spike. It was observed that ARG 493 of spike was making contact with GLU35, ASP38, and ASP355 of hACE2 for around 22 % of simulation time, and ASN487 of spike was making contact with TYR83 for 34 % of simulation time. Similarly, THR500 was making contact with ASP355 and TYR41 for 22 % of the simulation time, TYR449 was making contact with ASP38 for 22 % of simulation time, and ALA475 was making contact with SER19 for 24 % of simulation time. In contrast, in the case of WT spike-hACE2 interactions, the interactions were few in comparison to the Omicron spike. In the WT spike-hACE2 complex, ASN487 was making contact with TYR83 for 50 % of simulation time, THR500 was making contact with ASP355 for 42 % of simulation time, TYR489 was making contact with TYR83 for 49 % of the simulation time, and GLN493 was making contact with LYS31 for 20 % of simulation time (Fig. 3A and B).

Further, in both the complexes, ASN487, THR500 and GLY502 of spike protein were making hydrogen bond contacts with TYR83, ASP355 and LYS353, respectively. Besides that, TYR449 and ALA475 were involved in significant hydrogen bonding with ASP38 and SER19 of hACE2 in the Omicron-spike-hACE2 complex. While TYR489 was making a hydrogen bond with TYR83 in the WT-spike-hACE2 complex (Fig. 3A–D). Finally, to investigate the effect of the individual mutations

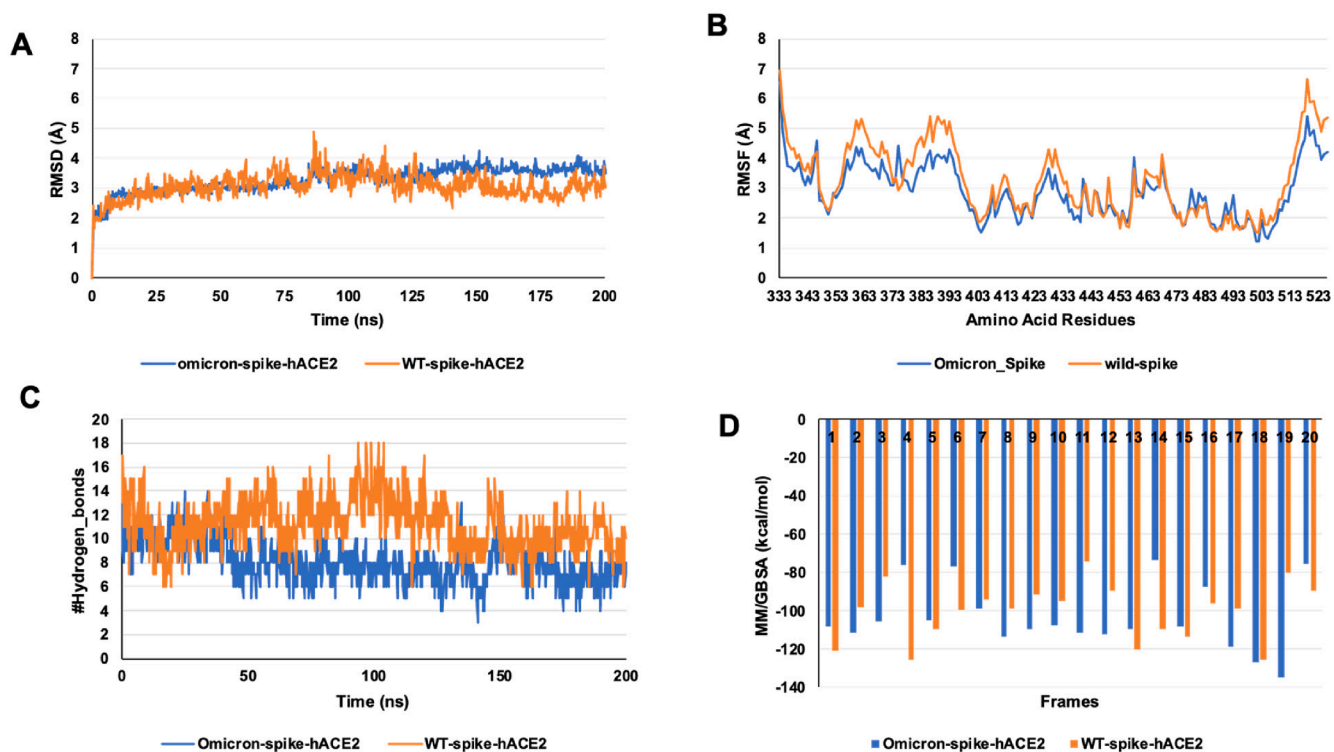


Fig. 2. The MD analysis of the simulated complexes. (A) The RMSD plot shows a similar deviation in the Omicron-spike-hACE2 and WT-spike-hACE2 complex. (B) The RMSF plot reveals that the Omicron-spike variant was more stable than the WT spike. (C) The number of hydrogen bond contacts was greater in the WT-spike-hACE-2 than in the Omicron-spike-hACE2 complex. (D) MM/GBSA binding free energy of the 20 structure complexes extracted from each trajectory at equal span, suggesting that both WT and Omicron spike had similar affinity for hACE2.

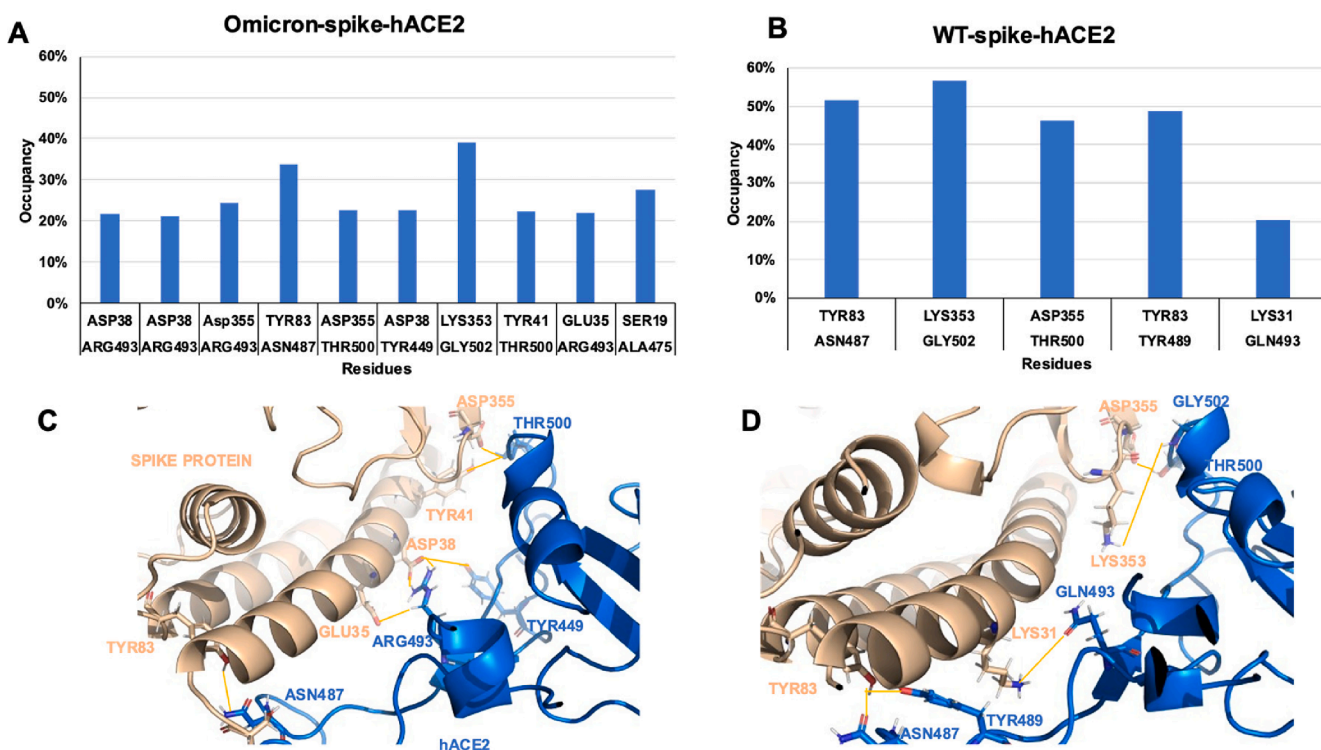


Fig. 3. Significant hydrogen bond contacts between the spike protein and hACE2. (A) The spike residues of the Omicron (RBD) variant (residues lower in the X axis) making hydrogen bond contacts with hACE2 (residues above in the X axis). (B) The WT spike hydrogen bond contact frequency with hACE2 (duplication of residue numbers is due to different hydrogen bonds within the same set of residues but between different atoms). (C) The ribbon representation of Omicron spike significant hydrogen bonds with hACE2. (D) The ribbon representation of WT spike significant hydrogen bonds with hACE2.

on the spike protein stability, the average structure from the last 100 ns of the simulation was extracted. The energy contribution of each mutated residue was calculated and compared with WT, and the energy difference has been shown in Fig. 4. In most of the cases, WT residues were favorable, while in the case of K417N, S477N, T478K, and Y505H modelled mutant residues were highly favorable (Fig. 4).

3.2. E484A mutation in the Omicron spike (RBD) has significantly decreased the binding energy and alters the fraction of H-bond interactions with neutralizing antibody

The wildtype (WT) spike-antibody complex and the Omicron spike-antibody complex were simulated for the 200 ns. The global deviation of the complexes with time was analyzed initially by calculating the RMSD. The RMSD data showed that within the first 100 ns of the simulation, both the complexes got stabilized. However, there was a difference in the average deviation, the WT-spike-antibody complex was found to be less deviating and stabler than the Omicron-spike-antibody complex. i.e., WT-spike-antibody ($3.74 \pm 0.52 \text{ \AA}$) and Omicron-spike-antibody ($6.64 \pm 1.05 \text{ \AA}$) (Fig. 5A). When the average fluctuation of the individual residues of the WT spike and Omicron spike protein was analyzed through RMSF calculation, it was found that Omicron spike residues and WT spike had similar average fluctuation. The average RMSF of the WT spike was $1.37 \pm 0.596 \text{ \AA}$, while for the Omicron spike it was $1.41 \pm 0.66 \text{ \AA}$. It was also observed that the residues 453–483 of Omicron had higher fluctuation than WT at the binding region for the neutralizing antibodies (Fig. 5B). To clearly understand the variations observed in the RMSD and RMSF plot, the number of hydrogen bonds between the spike-antibody in both the modelled mutants and wild type

was calculated. It was found that the WT spike-antibody (8.49 ± 1.50) had a higher number of hydrogen bonds throughout the simulations than the Omicron spike-antibody (6.32 ± 2.87) however when the number of hydrogen bonds were compared in the converged region between 100 ns and 200 ns the average number of bonds for WT spike-antibody (7.91 ± 1.63) found to be slightly lower than the Omicron spike-antibody (8.73 ± 1.71) (Fig. 5C). Further, the MM/GBSA free binding energy of the spike-antibody complex was computed by extracting 20 structures from the equal interval from the last 100 ns of the simulations. The binding free energy of each of the 20 structure complexes has been shown in (Fig. 5D). The individual binding energy for each structure along with all the energy terms contributing to overall MM/GBSA binding free energy has been reported in [supplementary material \(Table S1\)](#). The average free binding energy showed that Omicron-spike mutations had reduced the binding affinity to $(-57.76 \pm 19 \text{ kcal/mol})$ with antibody compared to WT-spike protein had a higher binding affinity $(-84.31 \pm 17 \text{ kcal/mol})$ for antibody. Then, the significant ($>20\%$ of simulation time) hydrogen bonding residues of spike protein with antibody and their contact frequency were calculated. It was found that the Omicron spike variant had less significant hydrogen bonding with antibody than the WT spike. It was seen that LYS484 in the Omicron variant had significantly decreased the hydrogen bond contacts, it was making no hydrogen bonding with antibody for a significant time duration, while GLU484 in WT was making one hydrogen bond each with ASN33 (29 % of simulation time), TYR34 (62 % of simulation time) and ARG112 (80 % of simulation time) of antibody respectively (Fig. 6A and B).

Further, in both the complexes, ASN450 of spike protein was involved in making hydrogen bond contacts with antibody; however, it

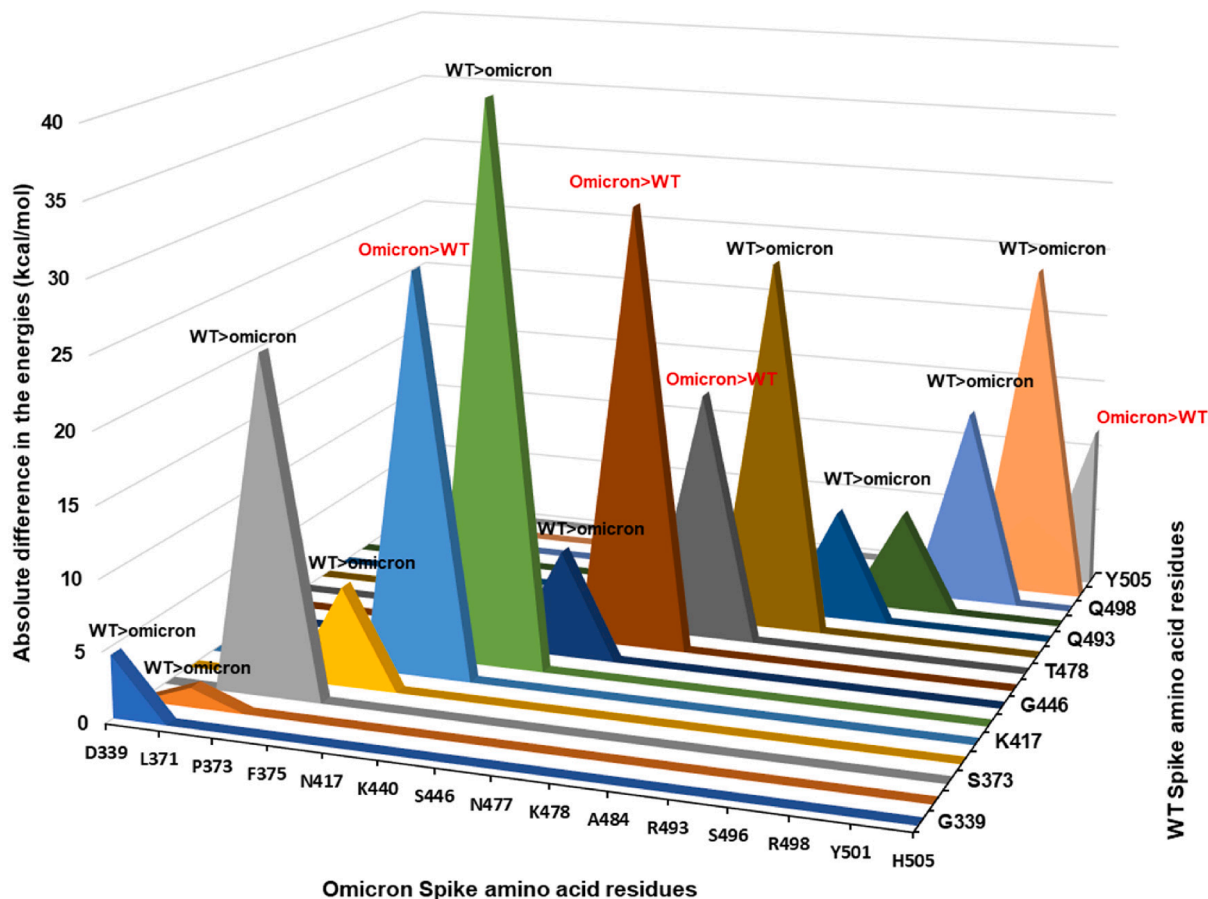


Fig. 4. The energy difference between the Omicron-modelled mutant residues compared to the WT spike. The energy differences are shown in the absolute values, the >sign represents the more favorable energy (more negative energy values) for the individual residues. Here, only position-specific comparisons have been made with each other, and not a single residue with all other residues.

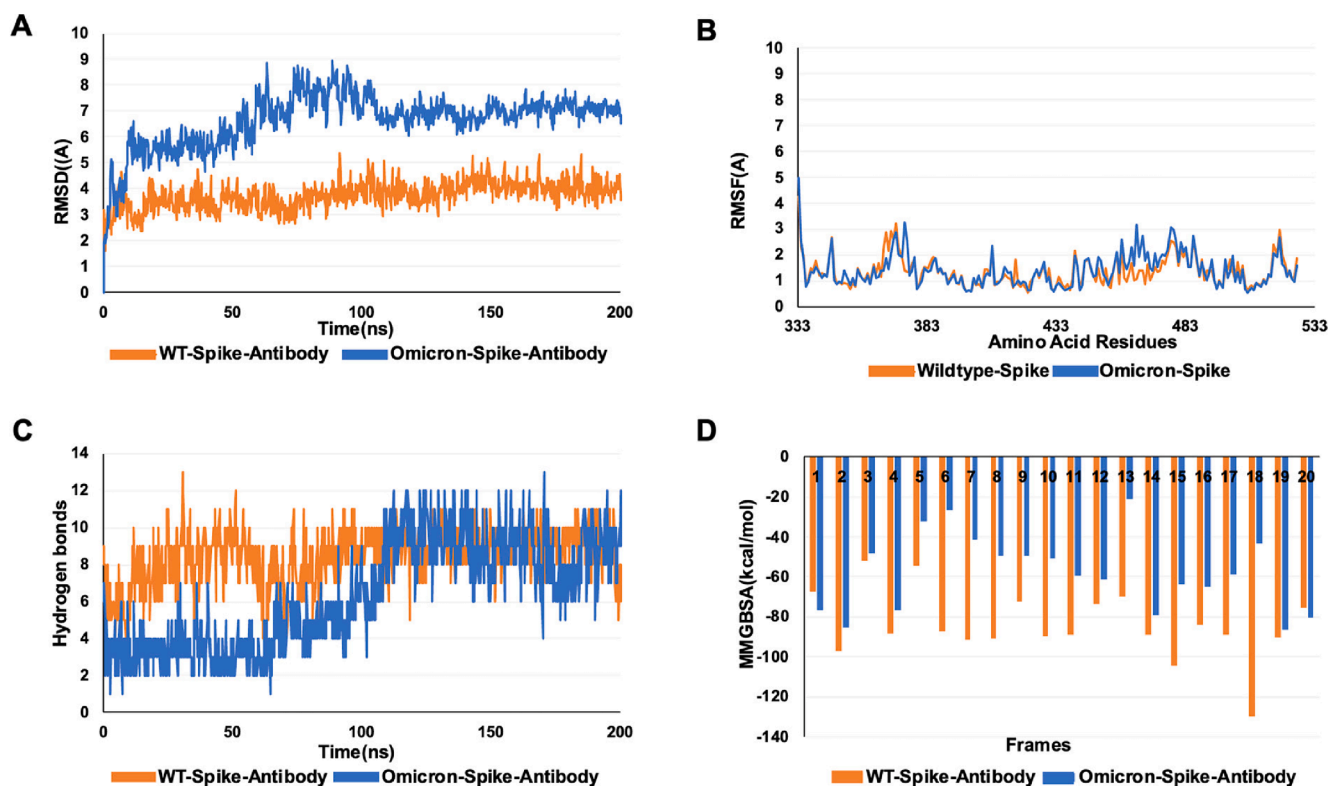


Fig. 5. The MD analysis of the simulated complexes. (A) The RMSD plot shows the unsimilar but stable deviation in the Omicron-spike-antibody and WT-spike-antibody complex. (B) The RMSF plot reveals that the WT-spike variant was more stable than the Omicron-spike in the region between residues 453–483. (C) The number of hydrogen bond contacts was greater in the WT-spike-Omicron than the Omicron-spike-antibody complex initially but got similar after the 100 ns simulation. (D) MM/GBSA binding free energy of the 20 structure complexes extracted from each trajectory at equal span, suggesting that WT spike protein has increased affinity for antibody compared with Omicron spike.

interacts with different residues GLY102 in Omicron spike-antibody complex and SER31 in wildtype spike-antibody complex. Apart from that, ASN481 and GLU471 were involved in significant hydrogen bonding with ARG111 and TYR93 of antibody in Omicron-spike-antibody complex only. While GLU484 was making double hydrogen bonds with ARG112 in WT-spike-antibody complex (Fig. 6A–D). Overall, the study indicates the lesser stability and lower binding affinity of the Omicron variant with neutralizing antibody compared to WT.

4. Discussion

Since the emergence of the SARS-CoV-2, it is constantly mutating and giving rise to different variants. Moreover, some variants emerged as VOC, namely Alpha, Beta, Delta and Omicron, which have caused multiple deadly waves in different nations. Alpha, the first variant discovered in the UK in September 2020, had four different mutations (H69-, V70-, N501Y and D614G) in the spike region of the virus (Aleem et al., 2021). After Alpha, the Beta variant of the SARS-CoV-2 was found in the population of South Africa in October 2020. It has five major mutations (L18F, K417N, E484K, N501Y and D614G) in the spike region, which were helpful in the higher transmission of the virus (Aleem et al., 2021). In March 2021, the Delta variant was discovered in India, bringing a second wave to the country and taking millions of lives (Kar et al., 2021). As of July 2021, the variant had been detected in more than 130 countries (<https://gyn.org/covid-19/delta-b-1-617-2/>). This variant has five major mutations (L452R, T478K, D614G, P681R and D950N), which were linked to its higher transmission and virulence (Kannan et al., 2021; Kumar et al., 2021; Liu et al., 2021a). Finally, the most recent VOC announced by WHO on 26 November 2021 was Omicron. The Omicron variant has A67V, Δ69-70, T95I, G142D/Δ143-145, Δ211/L212I, G339D, S371L, S373P, S375F, K417N, N440K, G446S,

S477N, T478K, E484A, Q493R, G496S, Q498R, N501Y, Y505H, T547K, D614G, H655Y, N679K, P681H, N764K, D796Y, N856K, Q954H, N969K, L981F mutations in the spike region of the virus (Callaway and Ledford, 2021; Chen et al., 2021; Sadek et al., 2021). Interestingly, the mutation N501Y has been conserved in most of these VOCs, namely alpha, beta and Omicron. In the previous study, it was reported that N501Y mutation caused a reduction in the binding affinity with neutralizing antibodies from the convalescent sera of the COVID-19-recovered patients compared to WT (Sabino et al., 2021; Wang et al., 2021; Williams and Zhan, 2021).

Further, multiple studies have shown that N501Y mutation has enhanced the binding affinity of the spike protein with hACE2 (Kumar et al., 2021; Leung et al., 2021; Liu et al., 2021b; Singh et al., 2021). The mutation E484K in the beta variant of the spike protein has been reported to aid the resistance towards various individual monoclonal antibodies to the RBD motif of the spike (Wang et al., 2021). Similarly, in Omicron, E484A mutation has been found, as no experimental study has been shown to investigate the effect of E->A mutation at the 484th position. However, this computational study suggests a reduction of affinity towards anti-RBD neutralizing antibody through the reduction of significant hydrogen bonding due to this mutation (Fig. 6 A-B). Further, P681R is conserved from delta to Omicron variant, and P681R mutation is at the furin cleavage site of the spike protein and has been shown to enhance the entry of the virus inside the human cells in delta variant in comparison to alpha and WT (Liu et al., 2021a). Altogether, all the previous studies had indicated an increase in the binding affinity and reduced affinity towards the individual antibodies in beta and delta variants. However, all the available vaccines have been shown to provide optimum protection against the previously known variants (Krause et al., 2021). As in the Omicron variant, various other mutations are also present, and the current study is showing a slight decrease in affinity

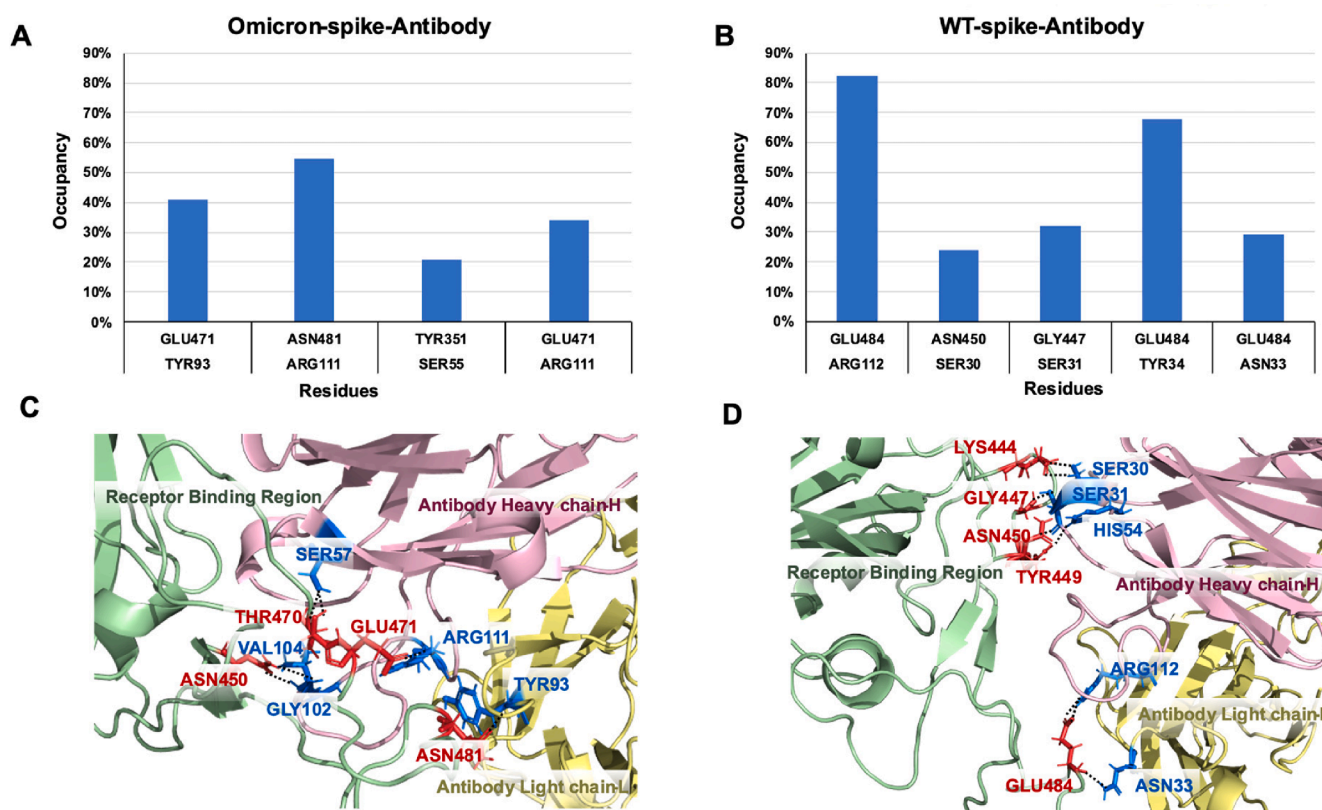


Fig. 6. Significant hydrogen bond contacts between the spike protein and antibody. (A) The spike residues of Omicron (RBD) variant (residues above in the X axis) making hydrogen bond contacts with antibody (residues lower in the X axis). (B) The WT spike hydrogen bond contact frequency with antibody. (C) The 3D representation of Omicron spike significant hydrogen bonds with antibody heavy chain (purple colour) and antibody light chain (yellow colour). (D) The 3D representation of WT spike significant hydrogen bonds with both heavy and light chains of antibody. (For interpretation of the references to colour in this figure legend, the reader is referred to the web version of this article.)

against an anti-RBD neutralizing antibody from the recovered patient. Further, the study showed a similar binding affinity of Omicron with hACE2 compared to WT. However, we have not performed the study with any vaccine-specific antibodies.

In the current work, computational biophysical studies of the spike-hACE2 and a spike-anti-RBD neutralizing antibody of the Omicron variant have been performed and compared to the wild type. In the case of the spike-hACE2 interactions, all the biophysical parameters were found to be similar, i.e., global deviation of the structures, fluctuation of individual residues and even the binding affinity of the spike (RBD) with hACE2. One major difference found between the Omicron and WT spike binding with hACE2 was the modelled mutation at Q493R, because of this mutation, the hydrogen bond interactions in Omicron were found to be increased by 2–3 times as compared to the WT. However, a more detailed study is needed to investigate the impact of this increase in interaction on increasing the transmission and virulence of this variant. Further, when the spike interactions with neutralizing antibody were studied, there was an alteration in the hydrogen bonding residues with antibody for the Omicron spike (receptor binding region) when compared with the wildtype spike (receptor binding region) along with changes in the RMSD and RMSF plots. The major difference found between the Omicron and WT spike binding with antibody was the mutation at E484A, which has reduced the hydrogen bonding with ARG112, ASN33, and TYR34 of neutralizing antibody. This mutation might be the reason for the significant change in the pattern of hydrogen bonding as well as the decreased binding energy with the antibody. However, there are some new hydrogen bonds still formed, which might prevent complete detachment of antibody from the spike protein. Further experimental studies are needed to confirm the reduction in binding energy and interactions of the Omicron variant with an anti-RBD

neutralizing antibody.

5. Conclusions

In the current study, the MD study of 200 ns was performed to investigate and compare the binding interactions, energy, and dynamics of Omicron-spike (RBD) with hACE2 and a neutralizing antibody against WT. It was found that Omicron and WT have a similar binding affinity with hACE2, while the number of interactions significantly increased in the case of Omicron, and various mutated residues were found to provide stability to the spike protein. Further, in the case of spike-neutralizing antibody, it was found that WT (RBD) has a higher binding affinity towards antibody compared to Omicron (RBD), and the number of hydrogen bonds during the simulation was higher for the WT (RBD).

Author contributions

V.K. contributed to conception, computational analysis and manuscript writing; S.S. contributed to conception, computational analysis and manuscript writing D.S. contributed to conception, manuscript writing, funding and resources.

CRedit authorship contribution statement

Vipul Kumar: Writing – original draft, Methodology, Formal analysis, Data curation, Conceptualization. **Seyad Shefrin:** Writing – original draft, Visualization, Software, Formal analysis, Data curation. **Durai Sundar:** Writing – review & editing, Supervision, Resources, Project administration, Conceptualization.

Declaration of competing interest

The authors declare that they have no known competing financial interests or personal relationships that could have appeared to influence the work reported in this paper.

Data availability

Source data for all the figures are provided with the paper.

Appendix A. Supplementary data

Supplementary data to this article can be found online at <https://doi.org/10.1016/j.jsb.2024.108087>.

References

- Abdelrahman, Z., Li, M., Wang, X., 2020. Comparative review of SARS-CoV-2, SARS-CoV, MERS-CoV, and influenza a respiratory viruses. *Front. Immunol.* 11, 552909.
- Aleem, A., Akbar Samad, A.B., Slenker, A.K., 2021. Emerging Variants of SARS-CoV-2 and Novel Therapeutics against Coronavirus (COVID-19). *StatPearls, Treasure Island (FL)*.
- Boni, M.F., Lemey, P., Jiang, X., Lam, T.T., Perry, B.W., Castoe, T.A., Rambaut, A., Robertson, D.L., 2020. Evolutionary origins of the SARS-CoV-2 sarbecovirus lineage responsible for the COVID-19 pandemic. *Nat. Microbiol.* 5, 1408–1417.
- Callaway, E., Ledford, H., 2021. How bad is omicron? What scientists know so far. *Nature* 600, 197–199.
- Chen, J., Wang, R., Gilby, N.B., Wei, G.-W., 2021. Omicron (B. 1.1. 529): Infectivity, vaccine breakthrough, and antibody resistance. *arXiv preprint arXiv:2112.01318*.
- Cucinotta, D., Vanelli, M., 2020. WHO Declares COVID-19 a pandemic. *Acta Bio-Med.: Atenei Parmensis* 91, 157–160.
- Heinz, F.X., Stiasny, K., 2021. Distinguishing features of current COVID-19 vaccines: knowns and unknowns of antigen presentation and modes of action. *NPJ Vaccines* 6, 104.
- Humphrey, W., Dalke, A., Schulten, K., 1996. VMD – visual molecular dynamics. *J. Molec. Graphics* 14, 33–38.
- Jorgensen, W.L., Chandrasekhar, J., Madura, J.D., Impey, R.W., Klein, M.L., 1983. Comparison of simple potential functions for simulating liquid water. *J. Chem. Phys.* 79, 926–935.
- Kalra, R.S., Tomar, D., Meena, A.S., Kandimalla, R., 2020. SARS-CoV-2, ACE2, and hydroxychloroquine: cardiovascular complications, therapeutics, and clinical readouts in the current settings. *Pathogens* 9.
- Kalra, R.S., Kumar, V., Dhanjal, J.K., Garg, S., Li, X., Kaul, S.C., Sundar, D., Wadhwa, R., 2021. COVID-19-inhibitory activity of withanolides involves targeting of the host cell surface receptor ACE2: insights from computational and biochemical assays. *J. Biomol. Struct. Dyn.* 1–14.
- Kannan, S.R., Spratt, A.N., Cohen, A.R., Naqvi, S.H., Chand, H.S., Quinn, T.P., Lorson, C. L., Byrareddy, S.N., Singh, K., 2021. Evolutionary analysis of the delta and delta plus variants of the SARS-CoV-2 viruses. *J. Autoimmun.* 124, 102715.
- Kar, S.K., Ransing, R., Arafat, S.M.Y., Menon, V., 2021. Second wave of COVID-19 pandemic in India: Barriers to effective governmental response. *EClinicalMedicine* 36, 100915.
- Karim, S.S.A., Karim, Q.A., 2021. Omicron SARS-CoV-2 variant: a new chapter in the COVID-19 pandemic. *Lancet*.
- Krause, P.R., Fleming, T.R., Longini, I.M., Peto, R., Briand, S., Heymann, D.L., Beral, V., Snape, M.D., Rees, H., Ropero, A.M., Balicer, R.D., Cramer, J.P., Munoz-Fontela, C., Gruber, M., Gaspar, R., Singh, J.A., Subbarao, K., Van Kerkhove, M.D., Swaminathan, S., Ryan, M.J., Henao-Restrepo, A.M., 2021. SARS-CoV-2 variants and vaccines. *N. Engl. J. Med.* 385, 179–186.
- Kumar, V., Singh, J., Hasnain, S.E., Sundar, D., 2021. Possible Link between Higher Transmissibility of Alpha, Kappa and Delta Variants of SARS-CoV-2 and Increased Structural Stability of Its spike Protein and hACE2 Affinity. *Int. J. Mol. Sci.* 22.
- Leung, K., Shum, M.H., Leung, G.M., Lam, T.T., Wu, J.T., 2021. Early transmissibility assessment of the N501Y mutant strains of SARS-CoV-2 in the United Kingdom, October to November 2020. *Euro Surveillance: bulletin European sur les maladies transmissibles = European communicable disease bulletin* 26.
- Liu, Y., Liu, J., Johnson, B.A., Xia, H., Ku, Z., Schindewolf, C., Widen, S.G., An, Z., Weaver, S.C., Menachery, V.D., Xie, X., Shi, P.Y., 2021a. Delta spike P681R mutation enhances SARS-CoV-2 fitness over Alpha variant. *bioRxiv*.
- Liu, Y., Liu, J., Plante, K.S., Plante, J.A., Xie, X., Zhang, X., Ku, Z., An, Z., Scharton, D., Schindewolf, C., Menachery, V.D., Shi, P.Y., Weaver, S.C., 2021b. The N501Y spike substitution enhances SARS-CoV-2 transmission. *bioRxiv*.
- Lu, H., Stratton, C.W., Tang, Y.W., 2020. Outbreak of pneumonia of unknown etiology in Wuhan, China: the mystery and the miracle. *J. Med. Virol.* 92, 401–402.
- Madhavi Sastry, G., Adzhigirey, M., Day, T., Annabhimoju, R., Sherman, W., 2013. Protein and ligand preparation: parameters, protocols, and influence on virtual screening enrichments. *J. Comput. Aided Mol. Des.* 27, 221–234.
- Olsson, M.H., Sondergaard, C.R., Rostkowski, M., Jensen, J.H., 2011. PROPKA3: consistent treatment of internal and surface residues in empirical pKa predictions. *J. Chem. Theory Comput.* 7, 525–537.
- Ranney, M.L., Griffith, V., Jha, A.K., 2020. Critical supply shortages – the need for ventilators and personal protective equipment during the covid-19 pandemic. *N. Engl. J. Med.* 382, e41.
- Roos, K., Wu, C., Damm, W., Reboul, M., Stevenson, J.M., Lu, C., Dahlgren, M.K., Mondal, S., Chen, W., Wang, L., Abel, R., Friesner, R.A., Harder, E.D., 2019. OPLS3e: extending force field coverage for drug-like small molecules. *J. Chem. Theory Comput.* 15, 1863–1874.
- Sabino, E.C., Buss, L.F., Carvalho, M.P.S., Prete Jr., C.A., Crispim, M.A.E., Fraiji, N.A., Pereira, R.H.M., Parag, K.V., da Silva Peixoto, P., Kraemer, M.U.G., Oikawa, M.K., Salomon, T., Cucunuba, Z.M., Castro, M.C., de Souza Santos, A.A., Nascimento, V.H., Pereira, H.S., Ferguson, N.M., Pybus, O.G., Kucharski, A., Busch, M.P., Dye, C., Faria, N.R., 2021. Resurgence of COVID-19 in Manaus, Brazil, despite high seroprevalence. *Lancet* 397, 452–455.
- Sadek, A., Zaha, D., Ahmed, M.S., 2021. Structural insights of SARS-CoV-2 spike protein from delta and omicron variants. *bioRxiv* 2021.2012.2008.471777.
- Schrödinger Release 2020-2. Protein Preparation Wizard, Epik, Impact, LigPrep, Glide, Schrödinger, LLC, New York, NY, 2020; Desmond Molecular Dynamics System, D. E. Shaw Research, New York, NY, 2020. Maestro-Desmond Interoperability Tools, Schrödinger, New York, NY, 2020. 2nd ed.
- Singh, J., Samal, J., Kumar, V., Sharma, J., Agrawal, U., Ehtesham, N.Z., Sundar, D., Rahman, S.A., Hira, S., Hasnain, S.E., 2021. Structure-function analyses of new SARS-CoV-2 Variants B.1.1.7, B.1.351 and B.1.1.28.1: clinical, diagnostic, therapeutic and public health implications. *Viruses* 13.
- Venkatakrishnan, A., Anand, P., Lenehan, P.J., Suratekar, R., Raghunathan, B., Niesen, M.J., Soundararajan, V., 2021. Omicron variant of SARS-CoV-2 harbors a unique insertion mutation of putative viral or human genomic origin.
- V'kovski, P., Kratzel, A., Steiner, S., Stalder, H., Thiel, V., 2021. Coronavirus biology and replication: implications for SARS-CoV-2. *Nat. Rev. Microbiol.* 19, 155–170.
- Wang, P., Nair, M.S., Liu, L., Iketani, S., Luo, Y., Guo, Y., Wang, M., Yu, J., Zhang, B., Kwong, P.D., Graham, B.S., Mascola, J.R., Chang, J.Y., Yin, M.T., Sobieszczyk, M., Kyrtsov, C.A., Shapiro, L., Sheng, Z., Huang, Y., Ho, D.D., 2021. Antibody Resistance of SARS-CoV-2 Variants B.1.351 and B.1.1.7. *bioRxiv*.
- Williams, A.H., Zhan, C.G., 2021. Fast prediction of binding affinities of the SARS-CoV-2 spike protein mutant N501Y (UK variant) with ACE2 and miniprotein drug candidates. *J. Phys. Chem. B* 125, 4330–4336.
- Ye, Z.W., Yuan, S., Yuen, K.S., Fung, S.Y., Chan, C.P., Jin, D.Y., 2020. Zoonotic origins of human coronaviruses. *Int. J. Biol. Sci.* 16, 1686–1697.
- Zeyaulah, M., AlShahrani, A.M., Muzammil, K., Ahmad, I., Alam, S., Khan, W.H., Ahmad, R., 2021. COVID-19 and SARS-CoV-2 Variants: current challenges and health concern. *Front. Genet.* 12, 693916.